Analyst

Accepted Manuscript

This article can be cited before page numbers have been issued, to do this please use: R. Ayyanu and P. Perumal, *Analyst*, 2019, DOI: 10.1039/C8AN02363H.

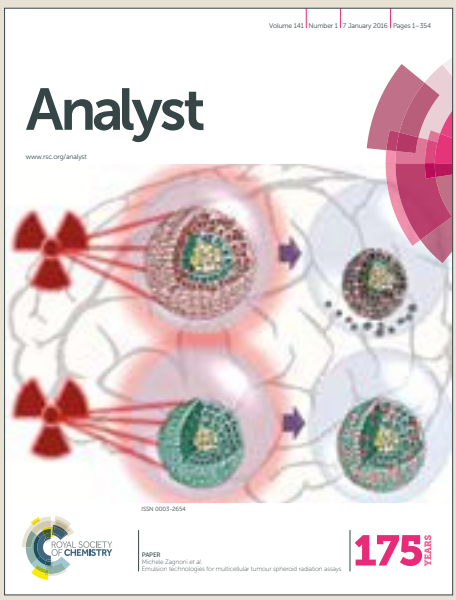

ROYAL SOCIETY OF CHEMISTRY

rsc.li/analyst

View Article Online
DOI: 10.1039/C8AN02363H

A novel fluorescent sensing platform based Metal-Polydopamine Frameworks for dual Detection of Kanamycin and Oxytetracycline

A.Ravikumar and P. Panneerselvam*

Department of Chemistry, SRM Institute of Science and Technology, Kattankulathur- 603 203,

Tamil Nadu, India.

*Corresponding author and E-mail address: panneerselvam.pe@ktr.srmuniv.ac.in, panneerchem82@gmail.com

View Article Online
DOI: 10.1039/C8AN02363H

Abstract

In this report, we have presented for the first time about dual detection of kanamycin (KMY) and oxyteracycline (OTC) using metal polydopamine frameworks (MPDA). This sensing system represents the metal polydopamine frameworks (MPDA) which act as a fluorescent quencher between the interaction the MPDA and dye labeled DNA molecules. The metal polydopamine frameworks exhibited an excellent fluorescent quenching behaviour and good analytical response towards the detection of biomolecules for KMY and OTC. The accumulation of kanamycin and oxyteracycline into the sensing system was recovered and monitored the fluorescent intensity was changes at 525 and 583 nm. Under the optimal conditions, the proposed sensing system remarkably achieved for the highly sensitivity and selectivity detection of KMY and OTC with limit of detection of 304 pM and 481 pM respectively. The selectivity of the developed sensor was explored in the presence of competitive biomolecules. Moreover this sensing system demonstrates the great potential and versatile to rapid detection. In addition, this biosensor has been successfully evaluated for the dual detection of KMY and OTC in different real samples.

View Article Online
DOI: 10.1039/C8AN02363H

1. INTRODUCTION

The presence of antibiotics residues in animal food is a serious consequences for the food safety issue.[1-4] The antibiotics causes serious side effects in human health such as ototoxicity, neprotoxicity, liver damage, yellowing of teeth and allergic reactions in human body.[5-7] The most commonly used detection methods for antibiotics include high performance liquid chromatography, capillary electrophoresis, chemiluminescence, liquid chromatography tandem mass spectrometry, capillary electrophoresis and microchip capillary electrophoresis.[8-13] These methods are highly expensive, time consuming, very difficult to sample preparation and more importantly sensitivity of in these methods are not sufficient. Therefore, highly sensitive, selective, rapid and cost effective methods for the detection of antibiotics are necessary to develop.

Now a day's colorimetric, electrochemical and fluorescent based biosensing methods are used for the detection of various analytes in environmental and biological applications.[14-16] However, the fluorescent based biosensor is one of the best analytical methods compared to other methods due to its very high sensitivity, rapid analysis and simplicity.[17] Since the most of the researchers focus on designed fluorescence based biosensor using labeled and label free single strand DNA (ssDNA) is selectively captured single target molecule. Even though the development of dual detection of biomolecules is very challenge compared to detection of single target molecule.[18-21] To date, the dual detection of biomolecules with high sensitivity is still remains a challenge.

Nanomaterials based fluorescent biosensors, owing to the advantages of high quenching efficiency, high sensitivity and detection limit is very high compared to other types of sensors.[22] As a class of nanomaterials, metal organic framework are very high quenching efficiency compared to other nanomaterials due to high surface area, electronic property, catalytic property and tunable nature.[23-26] Moreover, the MOF derivatives based on porous and hollow nanostructures, have been widely used various applications including energy storage, catalysis, drug delivery and biosensing.[27, 28] Recently, the MOFs with polydopamine based hollow nanomaterials of metal-polydopamine framework (MPDA) are used biosensor platform. Metal-polydopamine framework (MPDA) can be synthesized by under alkaline condition using MOFs act as a templates and in-situ polymerization of dopamine into polydopamine (PDA). Firstly, the

View Article Online
DOI: 10.1039/C8AN02363H

interaction between the organic ligands and metal ions, at the same time addition of dopamine is replaces the organic ligand and bind the metal ions due to metal ions and polydopamine bonding nature is highly stable than organic ligands and metal ions bonding nature. The main advantage of MPDA is it does not change it morphological structure after transformation of parent MOFs. Most importantly, the high surface area of MPDA is polymerization of PDA having plentiful functional groups. Therefore, MPDA are the suitable for biosensing platform and development for the detection of biomolecules.[29] The MPDA can absorb and quench dye-labeled single stranded DNA (ssDNA), when the absorbed ssDNA probes change the conformation structure to form double strand DNA (dsDNA) with its target molecule, the fluorescence is recovered because of ssDNA probes is released from surface of MPDA. In our previous work, we determine the fluorescence quenching efficiency of different fluorophore for the detection of Hg^{2+} and Ag^{+} ions using MPDA based sensing system.[30] This biosensing strategy is exhibited extremely high sensitivity and good quenching efficiency. Still now, for best of our the knowledge there are no report on the dual detection of kanamycin and oxytetracycline based on MPDA.

In this paper, we introduce a high quenching efficiency of MPDA with FAM and TAMRA labeled ssDNA for dual emission of fluorescent biosensing under 525 and 583 nm, which could be used to detect the KMY and OTC. The FAM and TAMRA labeled ssDNA is strongly adsorbed on the surface of MPDA. The MPDA serves as an efficient quencher for FAM and TAMRA labeled ssDNA without fluorescence signal. Then the addition of KMY and OTC in this sensing system, which could be interacted on the fluorophore labeled ssDNA and recover fluorescence intensity. The design of our biosensing platform exhibits high sensitive and selective detection of KMY and OTC and applied for environmental monitoring.

2. EXPERIMENTAL

2.1. Reagents and apparatus

OTC aptamer and KMY aptamer were obtained from integrated DNA technologies (IDT, Avantor, India). The sequence of

KMY aptamer: 5'-FAM-TGGGGGTTGAGGCTAAGCCGA-3,

OTC aptamer: 5'-TAMRA-GGAATTCGCTAGCACGTTGACGCTGGTGCCCGGTTGTGGT GCGAGTGTTGTGTGGATCCGAGCTCCACGTG-3′.

View Article Online
DOI: 10.1039/C8AN02363H

Standard oxytetracycline, kanamycin, tetracycline, streptomycin, DOX and amplcillin compounds were bought from Sigma Aldrich (India). Cobalt nitrate, 2-methyl imidazole, methanol and tris (hydroxymethyl) aminomethane were purchased from Alfa Aesar (India). All other solutions were prepared by double distilled water.

A Fluoromax-4 Spectrofluorometer (HORIBA scientific, France) was used for the fluorescence measurements. The fluorescence intensity of samples was measured at different excitation and emission wavelengths with slit width of 10 nm. High resolution transmission electron microscopy (HRTEM) images were obtained from using a JEOL JEM-2000 microscope operating at 120 KV. Fourier transform infrared spectra (FT-IR) were recorded as Agilent Technologies FT-IR spectrometer (USA). The X-ray diffraction studies was surveyed on a PAN analytical, the Netherlands with Cu Ka radiation (λ=1.54 Å) at a voltage of 40 kV.

2.2. Synthesis of ZIF-67

The ZIF-67 was synthesized according to the previous reported procedure.[31] In brief, Co $(NO_3)_2.6H_2O$ (1.455g) and 2-methylimidazole (1.65g) were dissolved in 30 mL of methanol separately. After that, the resulting above solutions was immediately mixed and vigorous stirred for 3h at room temperature. Finally, the obtained purple ZIF-67 were collected by centrifugation and washed three times with deionized water and methanol, and dried at 60 ^oC for further use.

2.3. Synthesis of Hollow Metal-polydopamine Framework (MPDA)

Hollow metal-polydopamine framework was synthesized by previously reported procedure.[32] Firstly, above prepared ZIF-67 (10 mg) was dispersed in a mixed solution of ethanol (20 mL) and water (15 mL) under ultrasonication. Then addition of dopamine hydrochloride (4 mg) was added in to the above solution under vigorous stirring for 5 min and then 10 mL of Tris-HCl buffer solution (20 mM, pH=8.5) was added in the mixture and reacted 48 h at room temperature under stirring. Finally, the resultant black coloured precipitate (denoted as "MPDA") was collected by centrifugation and washed with ultrapure water and ethanol separately.

View Article Online
DOI: 10.1039/C8AN02363H

2.4. Fluorescence assay for detection of kanamycin and oxytetracycline

The following detection experiments solutions were prepared in 20 mM Tris-buffer (pH 7.6, 60 μM $MgCl_2$, 75 mM NaCl). Firstly, the FAM-labeled KMY-specific oligonuclotide probe solution and TAMRA-labeled OTC-specific oligonuclotide probe solution were mixed in the buffer solution and then incubated for 5 min at 90 ^oC. After that the solution was slowly cooled down at room temperature. For kanamycin detection, 900 μL of above prepared mixed solution was taken in the 1.5 mL plastic vial and then added to 50 μL of 8 μg/mL MPDA solution and incubated for 10 min at room temperature. Then, different concentrations of kanamycin solution were added to the above reaction mixture. The solution was mixed well and incubated for 15 min at room temperature. Finally, the fluorescence intensity was measured by the excitation and emission wavelength at 480 nm and 525 nm respectively.

For oxytetracycline detection, the experimental procedure was similar to that of the detection of kanamycin. The fluorescence intensity was monitored by the excitation and emission wavelength at 530 nm and 583 nm respectively.

2.5. Real sample analytical procedure

The liquid dairy milk samples were collected from local supermarket nearer to SRMIST campus. The milk sample (5 mL), acetonitrile (7 mL) and trichloroacetic acid (10 mL) were added into a centrifuge tube and shaken continuously for 20 min to dissolve the organic substances and settle down the protein. After that, the mixed milk samples centrifuged for 5 min at 12,000 rpm. The middle liquid layer was separated and diluted for 5-fold concentrations with Tris-HCl buffer and then subjected to analytical procedure according to the above mentioned optimized conditions.

3. RESULTS AND DISCUSSIONS

3.1. Characterization of the hollow MPDA

Our synthesis of hollow metal polydopamine frame work through one-step transformation reaction begin with the addition of dopamine into a suspension of ZIF-67 in a mixture of solution ethanol and water. The hollow MPDA were synthesized by in-situ transformation process. The TEM image (Fig. 1A, B) of the obtained hollow MPDA exhibits a hollow structured morphology. The hollow MPDA maintained the polyhedral shape of ZIF-67 and formation of

View Article Online
DOI: 10.1039/C8AN02363H

hollow MPDA is coordination between Co^{2+} and PDA. The powder X-ray diffraction (XRD) patterns confirms that the hollow MPDA and ZIF-67. The predominant peaks belongs to the ZIF-67 completely disappeared in the MPDA (Fig.1C), indicating that the ZIF-67 was completely transformed into amorphous nature of MPDA. In addition, the FT-IR spectra were carried out to confirm the presence of functional groups in ZIF-67 and after the transformation product of MPDA as shown in Fig. 1D. The pure ZIF-67 exhibited two characteristic peaks at 1590 and 420 cm^{-1} corresponding to the stretching vibrations of C=N and Co-N group. After transformation of hollow MPDA exhibits three absorption peaks at 3200- 3400 $cm^{-1}$and 1590 cm^{-1}, which can be attributed to the stretching vibrations of O-H/N-H and ring vibration of indole respectively. Favorably, the above results indicate that successful synthesized by MPDA using the template of ZIF-67.

3.2. Sensing mechanism

We designed a two different fluorophore labeled ssDNA and hollow MPDA based sensing system used for the dual detection of kanamycin (KMY) and oxytetracycline (OTC) shown in scheme 1. The proposed sensing system is composed of mixing probes of KMY and OTC specific ssDNA, which were respectively labeled with FAM and TAMRA fluorophore. The FAM and TAMRA labeled ssDNA exhibit green and red fluorescence emission at 525 and 583 nm. The introduction of hollow MPDA in mixing probes of FAM and TAMRA labeled ssDNA brings significantly quenching of the fluorescence emission and exhibits low fluorescence signal. Because of the interaction between nucleobases and the surface of MPDA via π-π stacking interaction. The presence of KMY, preferentially binds the KMY specific aptamer due to hydrogen bonding interaction between the hydroxyl group in KMY and aptamer, which prevent the adsorption FAM labeled ssDNA and release the surface of MPDA. Consequently, the green colour (FAM) fluorescence recovered. Similarly, when introduce the OTC in mixing probes with MPDA, the OTC specific aptamer bind the OTC due to the electrostatic and hydrogen bonding effects on aptamer and OTC, The conformation change in OTC aptamer is removing the surface of MPDA, leading to recover the specific emission of red colour (TAMRA) fluorescence. As a result, the fluorescence change of the mixed mixing probes at 525 and 583 nm were monitored. Therefore, we developed a novel dual emission fluorescence sensing system for OTC and KMY using two dyes labeled target specific aptamer and hollow MPDA.

View Article Online
DOI: 10.1039/C8AN02363H

In addition, to investigate the detection feasibility of this sensing system is illustrated in Fig. 2a and b. The mixing probes of FAM labeled and TAMRA labeled ssDNA displays a strong fluorescence emission (Fig. 2aF_1 and bT_1). Upon the addition of hollow MPDA, the fluorescence intensity drastically decreased (Fig.2aF_2 and bT_2) due to rapid quenching effect of FAM and TAMRA labeled ssDNA. When adding kanamycin in this sensing system, change the conformation structure of ssDNA. It can be observed that the green colour (FAM) fluorescence emission is retained (Fig.2aF_3). At the same time, the red colour (TAMRA) emission is not retained (Fig.2bT_4). Similarly, the mixing probes with hollow MPDA sensing system of red colour (TAMRA) fluorescence emission retained upon oxytetracycline addition (Fig. 2bT_3) but no significant green fluorescence is observed (2aF_4). Furthermore, simultaneously addition of kanamycin and oxytetracycline in this sensing system to generates the green florescence emission from FAM at 525 nm and red florescence emission from TAMRA at 583 nm (Fig. 2aF_5 and bT_5). The intensity of fluorescence is similar to that of simultaneous and individual addition of kanamycin and oxytetracycline. To explain this phenonmenon, we measured the fluorescence intensity of this sensing system upon individually addition of kanamycin and oxytetracycline without interference each other. The above results demonstrated that the hollow MPDA with mixing probes sensing system can act as both individual and simultaneous detection of kanamycin and oxytetracycline.

3.3. Optimization of experimental conditions

To investigate the optimization of the proposed biosensing system can improve the sensitivity of the detection of kanamycin and oxytetracycline. Since the two different fluorophore attached ssDNA probes and binds hollow MPDA with high affinity, it is believed that the mixing ratio will weaken the release of ssDNA responding to target-ssDNA interactions. The mixing ratio between the two different dyes labeled ssDNA was optimized. As shown in Fig. 3a, decrease in the ratio of mixing probes resulted in a gradual decrease of fluorescence intensity and an increase the F/F_0. Therefore, to optimize the mixing ratio of two different dyes labeled ssDNA is 1:1 (50 nM of FAM labeled probe and 50 nM of TAMRA labeled probe).
Moreover, to evaluate the fluorescence quenching ability of the hollow MPDA, 10 nM of FAM and TAMRA labeled ssDNA was mixed with different concentrations of hollow MPDA ranging from 0 to 15 μg/mL (Fig. 3c and d). It can be observed that the FAM labeled ssDNA quenching

View Article Online
DOI: 10.1039/C8AN02363H

the saturated level is upon the addition of lower concentration of hollow MPDA (8 μg/mL), but TAMRA labeled ssDNA quenching the saturated level upon the addition of hollow MPDA upto 12 μg/mL. Therefore, 8 μg/mL of hollow MPDA was chosen as the optimal concentration for detection of kanamycin and oxytetracycline. In addition, the quenching kinetics of the proposed sensing system was investigated by detection of kanamycin and oxytetracycline. The fluorescence intensity of FAM and TAMRA labeled ssDNA was decreased by increasing the time and saturation after increasing the time of 8 min (Fig. 3d). The optimized quenching time was selected as 8 min for further experimental conditions. Moreover, we have developed a comparison of MPDA with graphene oxide (GO) for fluorescence quenching efficiency. As shown in Fig. 4, MPDA is effectively quenched the fluorescence of mixing probes of FAM and TAMRA labeled probes than GO. Because of polydopamine interacted with the Co^{2+} ion and formation of hollow MPDA.

3.4. Detection performance of the assay

To analyze the dual detection of antibiotics for kanamycin and oxytetracycline. As shown in Fig. 5a, increasing the concentrations of kanamycin in the range from 0 to 2 μM resulted in dramatic increase of fluorescence intensity, which was ascribed that change the conformation structure in the FAM labeled ssDNA. From the insert Fig. 5b, the linear relationship between the F/F_0 value and concentrations of kanamycin from 0 to 50 nM (R^2= 0.982). The limit of detection was calculated as 304 pM based on the 3σ method. Fig.6a shows the fluorescence responses to different concentrations of oxytetracycline. The fluorescence intensity was gradually increased from increasing concentrations of oxyteracycline. The linear relationship between the fluorescence intensity and concentrations oxytetracycline in the range from 0 to 50 nM (Insert Fig. 6b). The correlation coefficient value is R^2= 0.972 with the detection limit was estimated to be 481 pM by 3 σ method. The hollow MPDA based sensing system has superior sensitivity and many advantages of when comparable with the previously reported work of detecting of kanamycin and oxytetracycline (Table 1). This sensing system has very low detection limit compared to other sensing system for detection of kanamycin and oxytetracycline. We also would like to point out that very important advantage of our sensing system for dual detection of kanamycin and oxytetracycline with no need of masking agents. Even if, highly sensitive and

View Article Online
DOI: 10.1039/C8AN02363H

dual detection of kanamycin and oxytetracycline, can be clearly demonstrate to excellent performance.

Furthermore, we need to examine specificity of this sensing system toward four different interfering antibiotics (TET, DOX, streptomycin, ampicillin). The concentration of the other antibiotics was 5μM and concentrations of kanamycin and oxytetracycline is 50 nM. As shown in Fig. 7a and b, we tested for fluorescence intensity of four antibiotics with kanamycin and oxytetracycline. The kanamycin and oxytetracycline only response the fluorescent signal enhancement of F/F_0 values but other antibiotics having no fluorescence enhancement in this sensing system. These results indicate that the proposed sensing system did not interfere with other antibiotics.

3.5. Detection of kanamycin and oxytetracycline in real sample analysis

In order to study the practical application of the hollow MPDA based fluorescence biosensor for detection of kanamycin and oxytetracycline in real sample analysis of milk samples. The different milk samples were purchased from the supermarket. kanamycin and oxytetracycline spiked concentrations are 5 nM, 10 nM and 15 nM. The satisfactory recoveries of kanamycin and oxytetracycline samples ranged from 96% to 101% and 95% to 100% as shown in Table. 2. Hence, the results suggest that the developed sensing system can be applied to very high sensitive and selective detection of kanamycin and oxytetracycline in milk samples with acceptable accuracy, and suitable for practical use.

4. Conclusion

In this work, we have successfully developed a fluorescence sensing platform for dual detection of kanamycin and oxytetracycline. The proposed sensing system using the high fluorescence quenching capability of MPDA and specificity of FAM and TAMRA labeled ssDNA. The fluorescence intensity is monitored by after addition of kanamycin and oxytetracycline in this sensing system, which results kanamycin and oxytetracycline interact the dye labeled ssDNA and release the surface of hollow MPDA. This sensing method can achieve the detection limit is 304 pM and 481 pM for kanamycin and oxytetracycline, which was considerably lower than the detection limits of other type of sensors. In addition, the developed

View Article Online
DOI: 10.1039/C8AN02363H

sensing method was also applied for the detection of kanamycin and oxytetracycline in milk samples and good recovery results. Overall, the proposed sensing method was superior to most fluorescence biosensor for its simple, reliable, highly sensitive and selective detection of kanamycin and oxytetracycline and potentially expanded to other targets in environmental and biological applications.

Reference

1. K. De Wasch, L. Okerman, S. Croubels, H. De Brabander, J. Hoof and P. De Backer, Anayst, 1998, **123**, 2737-2741.
2. N. Furusawa, J. Vet. Med. A, 1999, **46**, 599-603.
3. R. Zeng, L. Su, Z. Luo, L. Zhang, M. Lu and D. Tang, Anal.Chim. Acta, 2018, **1038**, 21-28.
4. R. Zeng, Y. Tang, L. Zhang, Z. Luo and D. Tang, J. Mater. Chem. B, 2018, **6**, 8071-8077.
5. K. M. Song, H. Jo, K. Min, S. H. Jeon, T. Kim, M. S. Han, J. K. Ku and C. Ban, Anal. Biochem., 2011, **415**, 175-181.
6. R. Oertel, V. Neumeister and W. Kirch, J. Chromatogr. A, 2004, **1058**, 197-201.
7. Y. Jin, J. W. Jang, C. H. Han and M. H. Lee, J. Vet. Sci., 2006, **7**, 111-117.
8. J. W. Fritz and Y. G. Zuo, Food Chem., 2007, **105**, 1297-1301.
9. Y. X. Zhou, W. J. Yang, L. Y. Zhang and Z. Y. Wang, J. Liq. Chromatogr. Relat. Technol., 2007, **30**, 1603-1615.
10. M. Gbylik-Sikorska, A. Posyniak, T. Sniegocki and J. Zmudzki, Chemosphere, 2015, **119**, 8-15.
11. M. A. Bimazubute, E. Rozet, I. Dizer, J. C. V. Heugen, E. Arancio, P. Gustin, J. Crommen and P. Chiap, J. Chromatogr. B, 2009, **877**, 2349-2357.
12. M. Preu, D. Guyot and M. Petz, J. Chromatogr. A, 1998, **818**, 95-108.
13. A. V. Herrera-Herrera, L. M. Ravelo- Perez, J. Hemandez-Borges, M. M. Afonso, J. A. Palenzuela and M. A. Rodriguez-Delgado, 2011, J. Chromatogr. A, 2011, **1218**, 5352-5361.
14. M. Sierra-Rodero, J. M. Femandez-Romero and A. Gomez-Hens, Microchim Acta, 2014,**181**, 1897-1904.

View Article Online
DOI: 10.1039/C8AN02363H

15. F. Yuan, H. Zhao, Z. Zhang, L. Gao, J. Xu and X. Quan, RSC Adv., 2015, **5**, 58895-58901
16. K. H. Leung, Z. H. Daniel, S. H. Chan, W. C. Fu, C. H. Hang and L. D. Lungma, Sensor Actuat. B-Chem., 2013, **177**, 487-492.
17. Y. Zhu, P. Chandra, K. M. Song, C. Ban and Y. B. Shim, Biosensors and Bioelectronics, 2012, **36**, 29-34.
18. A. Ravikumar and P. Panneerselvam, Analyst, 2018, **143**, 2623-2631.
19. K. A. Rawat, H. Basu, R. K. Singl and S. K. Kailasa, RSC Adv., 2015, **199**, 19924-19932.
20. Q. Zhou, Y. Lin, M. Xu, Z. Gao, H. Yang and D. Tang, Anal. Chem., 2016, **88(17)**, 8886-8892.
21. Z. Qiu, J. Shu and D. Tang, Anal. Chem., 2017, **89(9)**, 5152-5160.
22. K. A. Rawat, K. R. Surati and S. K. Kailasa, Anal. Methods, 2014, **6**, 5972-5980.
23. X. Zuo, H. Zhang, W. Wang, J. Feng and X. Chen, Biosens. Bioelectron., 2016, **85**, 464-470.
24. K. Wang, D. Feng, T. F. Liu, J. Su, S. Yuan, Y. P. Chen, M. Bosch, X. Zou and H. C. Zhou, J. Am. Chem. Soc., 2014, **136**, 13983-13986.
25. S. S. Nagarkar, A. V. Desai and S. K. Ghosh, Chem. Eur. J., 2015, **21**, 9994-9997.
26. Z. Hu, B. J. Deibert and J. Li, Chem. Soc. Rev., 2014, **43**, 5815-5840.
27. X. Zhao, X. Bu, Q. G. Zhai, H. Tran and P. Feng, J. Am. Chem. Soc., 2015, **137**, 1396-1399.
28. T. Kiyonaga, M. Tomokazu, T. Kajiwara, J. Duan, K. Nagashima and S. Kitagawa, Chem. Commun., 2015, **51**, 2728-2730.
29. R. Ren, G. Cai, Z. Yu, Y. Zeng and D. Tang, Anal. Chem., 2018, **90(18)**, 11099-11105.
30. A. Ravikumar, P. Panneerselvam and N. Morad, ACS Appl. Mater. Interfaces, 2018, **10**, 20550-20558.
31. G. Yanna, T. Jing, Q. Huayu, W. Zhingli and Y. Yusuke, Chem. Mater. 2017, **29**, 5566-5573.
32. Y. Liang, J. Wei, Y. X. Hu, X. F. Chen, J. Zhang, X. Y. Zhang, S. P. Jiang, S. W. Tao and H. T. Wang, Nanoscale, 2017, **9**, 5323-5328.

View Article Online
DOI: 10.1039/C8AN02363H

33. R. Su, J. Xu, Y. Luo, Y. Li, X. Liu, J. Bie and C. Sun, Material Letters, 2016, **180**, 31-34.

34. D. Zheng, X. Zhu, X. Zhu, B. Bo, Y. Yind and G. Li, Analyst, 2013, **138**, 1886-1890.

35. Y. S. Kim, J. H. Kim, I. A. Kim, S. J. Lee, J. Jung and M. B. Gu, Biosens. Bioelectron., 2010, **26**, 1644-1649.

36. H. M. Zhao, S. Gao, M. Liu, Y. Y. Chang, X. F. Fan and X. Quan, Microchim Acta, 2013, **180**, 829-835.

37. Y. Wang, P. Ni, S. Jiang, W. D. Lu, Z. Li, H. Li, Y. Sun and Z. Li, Sensor Actuat. B-Chem., 2018, **254**, 1118-1124.

38. X. J. Bai, H. Hou, B. L. Zhang and J. L. Tang, Biosens. Bioelectron., 2014, **56**, 112-116.

39. Y. Zhu, P. Chandra, K. M. Song, C. Ban and Y. B. Shim, Biosens. Bioelectron., 2012, **36**, 29-34.

40. Y. P. Xing, C. Liu, X. H. Zhou and H. C. Shi, Sci. Rep, 2015, **5**, 8125.

View Article Online
DOI: 10.1039/C8AN02363H

FIGURE CAPTIONS

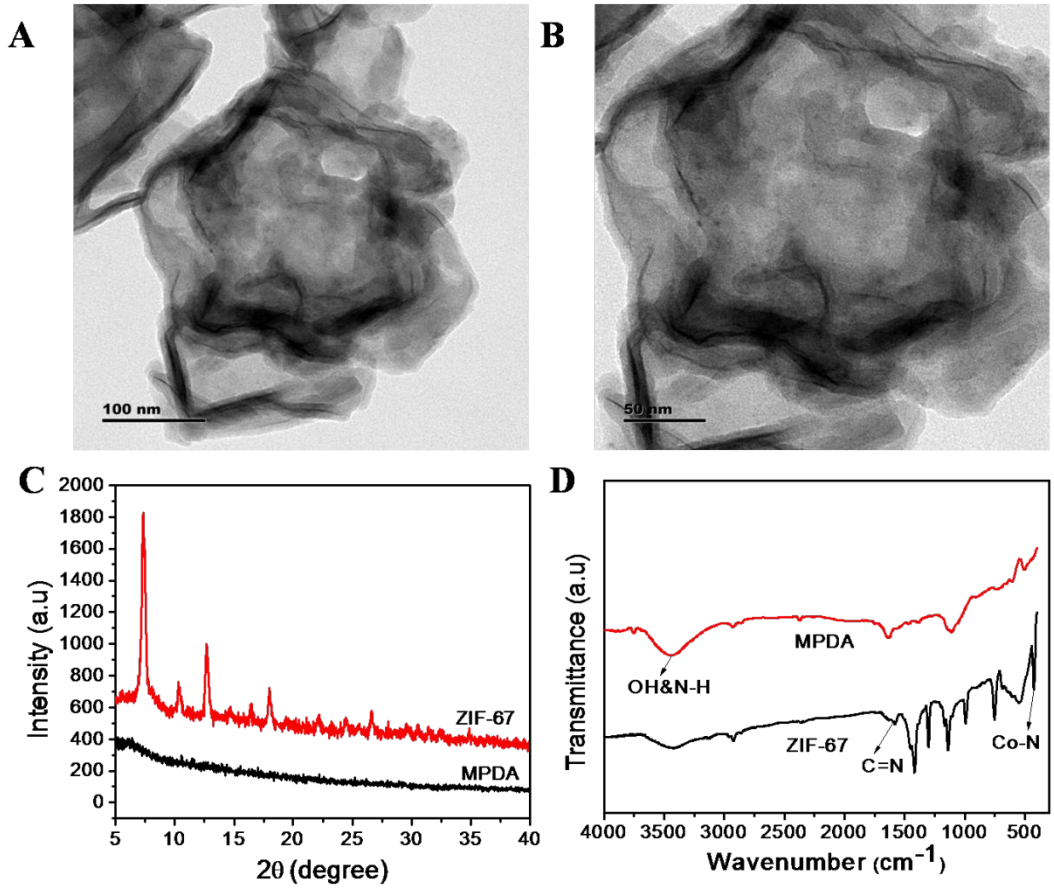

Fig.1. The characterization of hollow MPDA (A, B) HRTEM image of hollow MPDA, (C) PXRD pattern of ZIF-67 and hollow MPDA, (D) FT-IR spectra of ZIF-67 and hollow MPDA.

View Article Online
DOI: 10.1039/C8AN02363H

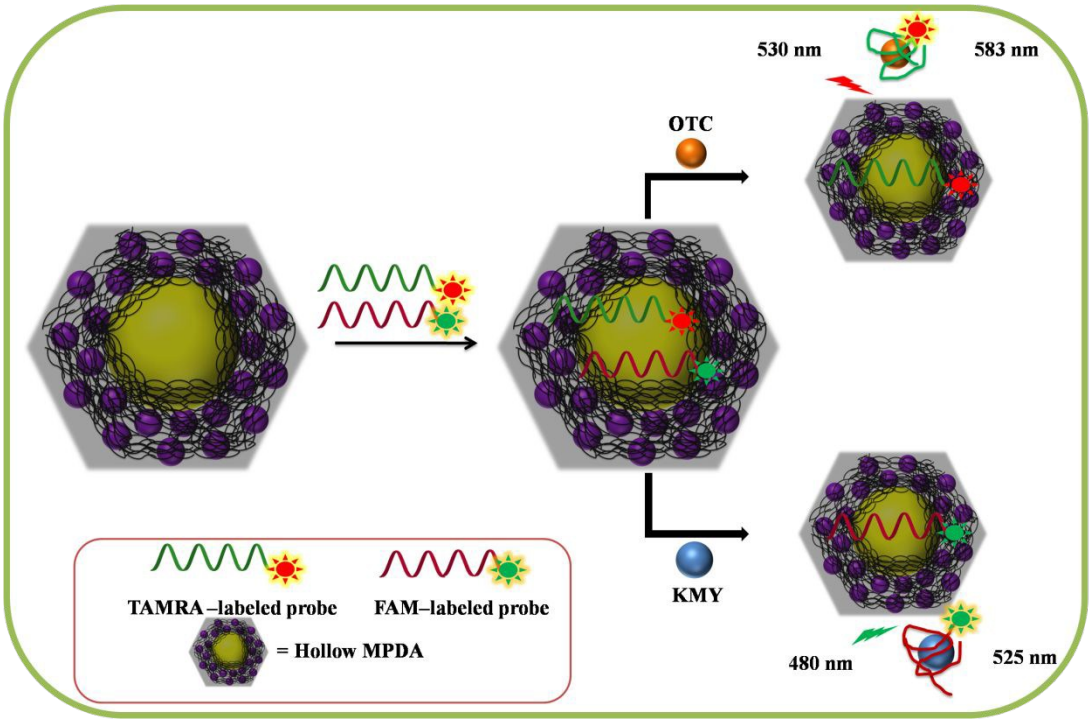

Scheme 1. Schematic illustration of the sensing principle of simultaneous detection of KMY and OTC based on hollow MPDA sensing system.

View Article Online
DOI: 10.1039/C8AN02363H

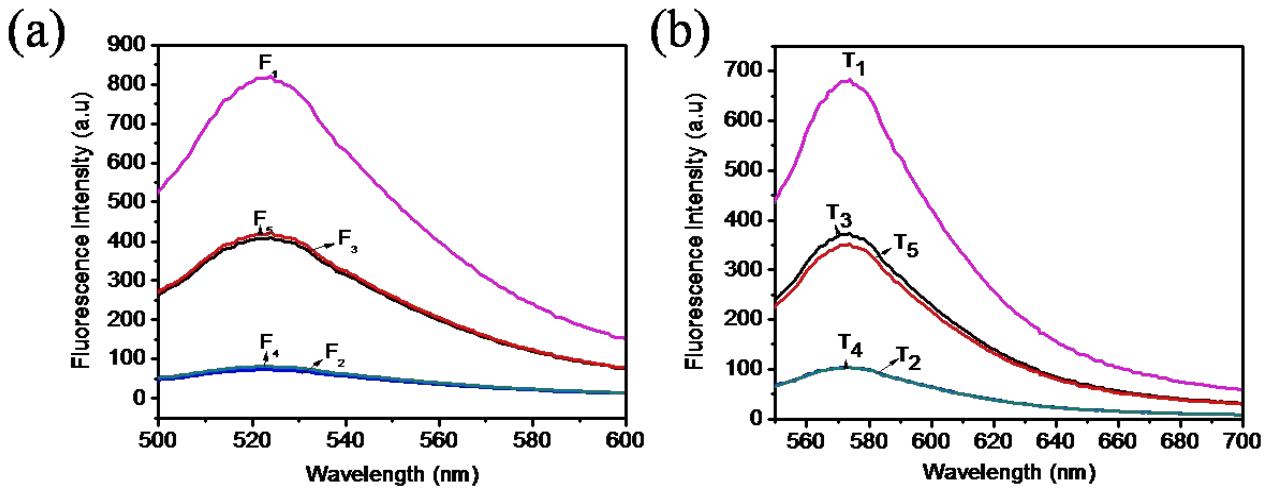

Fig. 2. The fluorescence spectra of detection of KMY and OTC (a) Fluorescence spectra of FAM labeled ssDNA with different conditions (F_1) mixing probes, (F_2) mixing probes with hollow MPDA, (F_3) mixing probes with hollow MPDA+KMY, (F_4) mixing probes with hollow MPDA+OTC, (F_5) mixing probes with hollow MPDA+KMY+OTC. (b) Fluorescence spectra of FAM labeled ssDNA with different conditions (T_1) mixing probes, (T_2) mixing probes with hollow MPDA, (T_3) mixing probes with hollow MPDA+KMY, (T_4) mixing probes with hollow MPDA+OTC, (T_5) mixing probes with hollow MPDA+KMY+OTC.

View Article Online
DOI: 10.1039/C8AN02363H

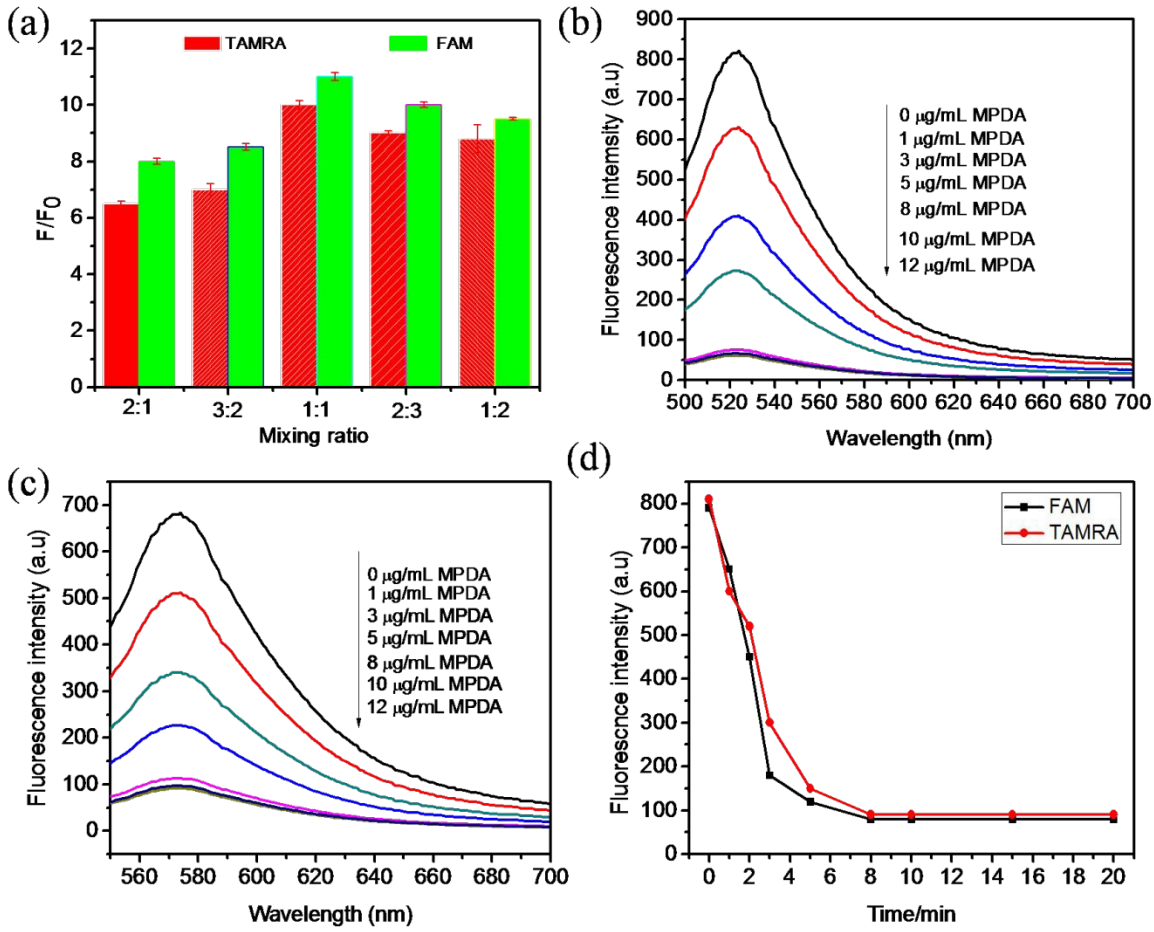

Fig. 3. (a) Fluorescence responses of hollow MPDA based sensing system with different FAM and TAMRA ratios in the presence of KMY and OTC, (b) The fluorescence emission spectra of different concentrations of hollow MPDA with FAM labeled ssDNA, (c) The fluorescence emission spectra of different concentrations of hollow MPDA with TAMRA labeled ssDNA, (d) The fluorescence quenching of FAM and TAMRA labeled ssDNA with hollow MPDA as a function of time.

View Article Online
DOI: 10.1039/C8AN02363H

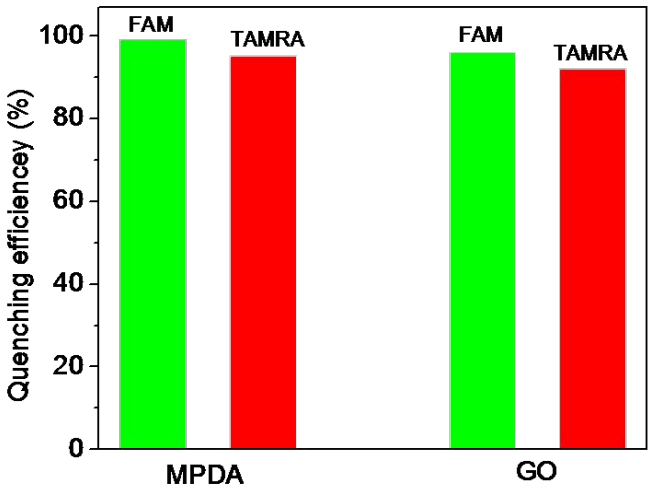

Fig. 4. Fluorescence quenching efficiency of MPDA and GO

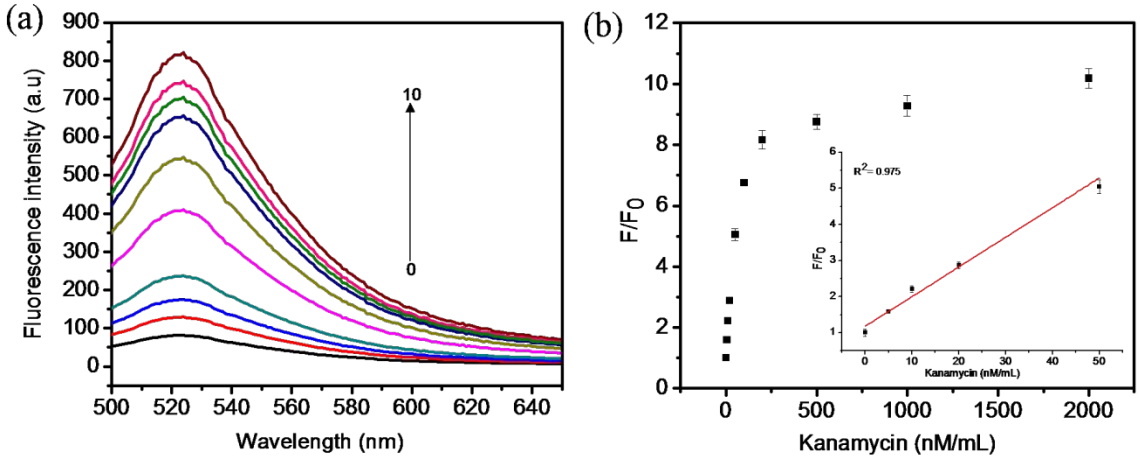

Fig. 5. Performance of the developed KMY biosensor (a) The produced fluorescence responses when different concentrations of KMY were tested, (b) Linear relationship between the fluorescence intensity and KMY concentration.

View Article Online
DOI: 10.1039/C8AN02363H

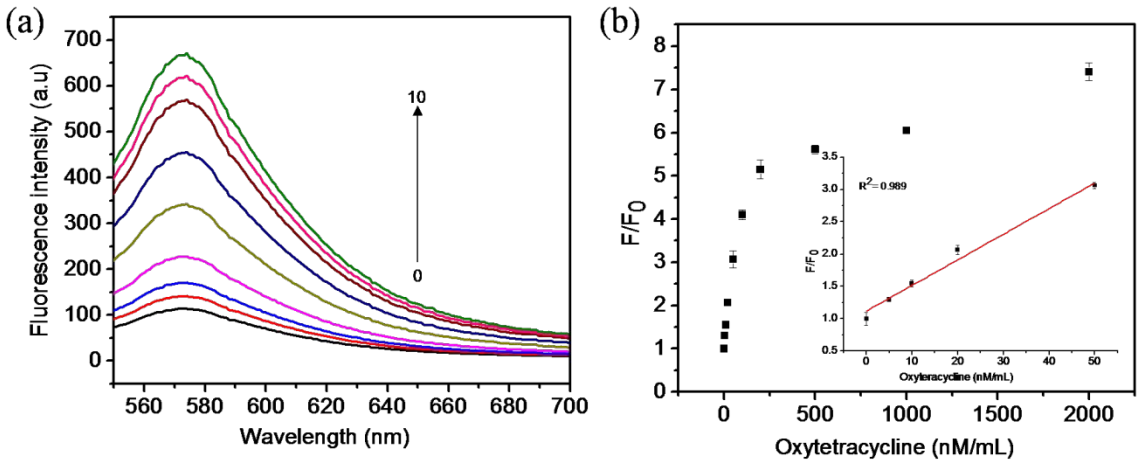

Fig. 6. Performance of the developed OTC biosensor (a) The produced fluorescence responses when different concentrations of OTC were tested, (b) Linear relationship between the fluorescence intensity and OTC concentration.

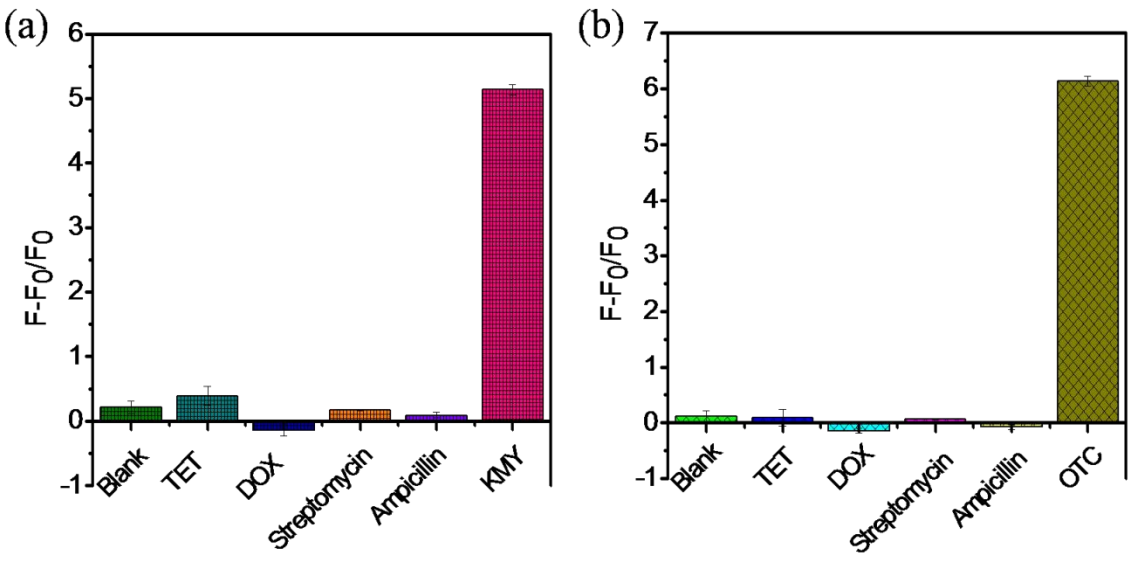

Fig.7. The selectivity of the developed biosensor (a) Selectivity of study KMY with other different antibiotics, (b) Selectivity of study KMY with other different antibiotics

View Article Online
DOI: 10.1039/C8AN02363H

Table 1 Comparison of other analytical methods for detection of KMY and OTC

.

Anaytical Methods	Target molecule	Linear range	LOD	Reference
Fluorescence	KMY OTC	0-2 μM	308 pM 408 pM	This work
Colorimetric	OTC	2-28 μg	0.227 μg	33
Electrochemical	OTC	10-600 ng	9.8 ng	34
Colorimetric	OTC	25-1000 nM	25 nM	35
Fluorescence	OTC	0.1-2 μM	10 nM	36
Fluorescence	OTC	25 nM- 1.75 μM	9.5 nM	37
Colorimetric	KMY	N/A	25 nM	5
Labe-free	KMY	100 μM-10 mM	50 μM	38
Label-free	KMY	0.05 μM-9 μM	9.4 nM	39
Fluorescence	KMY	0.1 μM-20 μM	59 nM	40

Table 2. Analysis of KMY and OTC in different milk samples

Samples	Spiked (nM)	Detected to KMY ±SD	Recovery (%)	Detected to OTC ±SD	Recovery (%)
Milk Sample 1	5	5.06 ± 1.12	101	5.09± 2.22	101.8
	10	10.26 ±1.21	102	9.50 ±1.89	95
	15	15.59 ± 2.2	103	15.20 ± 1.5	101
Milk Sample 2	5	4.9 ± 1.12	98	5.10± 1.02	102
	10	10.26 ±1.21	102	10.12 ±0.99	101
	15	15.03± 2.2	100	14.50 ± 0.52	96
Milk Sample 3	5	4.90± 2.22	101	4.80± 1.95	101.4
	10	9.30 ±0.99	96	10.16 ±1.56	101.6
	15	15.10 ± 1.2	100	14.80 ± 1.34	98.6

View Article Online
DOI: 10.1039/C8AN02363H

Graphical abstract